

Mean-Field Quantization of Several Hundred Electrons in Sodium Metal Clusters

S. Bjørnholm, J. Borggreen, O. Echt,^(a) K. Hansen, J. Pedersen, and H. D. Rasmussen

The Niels Bohr Institute, University of Copenhagen, DK-2100 Copenhagen Ø, Denmark

(Received 22 June 1990)

Measurements of the mass-abundance spectra of sodium clusters from supersonic expansions are presented. The spectra show evidence of a regular spherical shell structure with magic numbers N_0 scaling approximately with the cube root of the number of sodium atoms N , and hence the number of delocalized (valence) electrons in the cluster. Altogether twelve shell closings are observed, adding to the previously known shell closings, $N_0=2, 8, 20, 40, 58, 92$, and 138, the 8–12th magic numbers $N_0=196, 260, 344, 440$, and 558. The implications of shell structure in such large systems are discussed.

PACS numbers: 71.25.Lf, 03.65.-w, 35.20.Wg, 36.40.+d

The discovery by Knight *et al.* in 1984 of quantal shell structure in small droplets of sodium metal, with characteristic magic numbers, has opened new perspectives in the study of shell structure in many-fermion systems.¹ Previously these were confined to atoms and atomic nuclei. The perspective is widened by subsequent discoveries of similar shell structures in clusters of potassium,² cesium,³ copper, silver, gold,⁴ and other simple metals.

In a parallel development, mean-field theories^{5–7} based on methods borrowed from the description of simple metals in bulk form (jellium model) have led to a picture of the binding field of the valence electrons much like the nuclear mean field,⁸ except that the nuclear spin-orbit interaction is missing. Thus, the simple picture of conduction electrons moving freely and independently inside a metal, bounded only by the surface, seems to be valid down to the smallest sizes comprising less than one hundred atoms.

This Letter addresses the question of the extension of shell structure to larger sizes. Our approach is experimental. It gives substance to a recent theoretical study⁹ of the same problem.

The extension to sizes exceeding one hundred particles is interesting for several reasons. Viewing metal clusters as samples of bulk matter in embryonic form,¹⁰ the shell structure reflects a very special situation where the electron quantization is governed by the geometry of the surface, as opposed to the more normal situation, where it is the lattice that determines the bulk electron wave functions. It would be interesting to know the transition point between these two regimes. Shell structure in systems larger than atoms and nuclei is furthermore interesting because it offers an opportunity to pursue this phenomenon towards the limit of very large single-particle action quantum numbers, where one should be able to establish a correspondence between classical and quantal motion. Here, closed classical orbits of triangular and square shapes are expected to play a special role.

This subject is pursued in the theoretical study by Nishioka, Hansen, and Mottelson.⁹ It applies and ex-

tends ideas originally developed by Balian and Bloch,¹¹ and further by Bohr and Mottelson,¹² to the concrete case of electrons moving in a spherical Woods-Saxon potential with parameters appropriate to metallic sodium. In particular, the volume of the binding field is proportional to the number of constituents N in the cluster. Adding the single-particle energy eigenvalues of this potential leads to a sum $E(N)$, where the main trend is a (negative) volume term, proportional to the number of electrons N , and a (positive) surface term, proportional to $N^{2/3}$. Superimposed on this is an oscillating term, $E_{\text{shell}}(N)$. This quantity⁹ is presented in Fig. 1, where it is plotted as a function of the linear dimensions of the cluster, i.e., $\sim N^{1/3}$. The downward cusps represent shell closings, occurring at magic numbers. Our experimental results corroborate the mean-field, independent-particle assumptions and substantiate a prominent feature of this calculation, namely, the approximately equidistant spacing of shells, when expressed in terms of the linear dimensions.

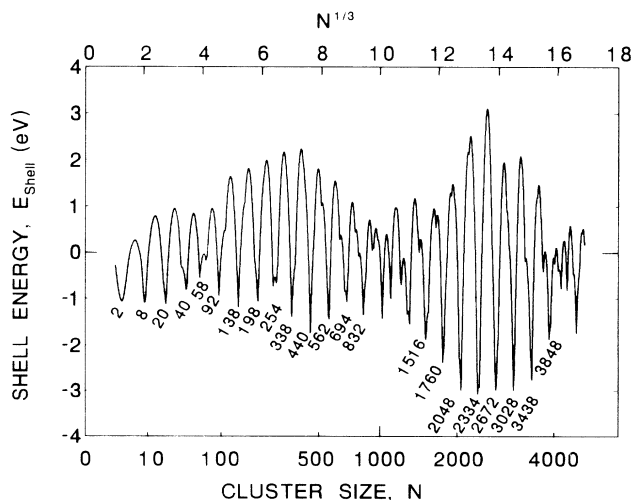


FIG. 1. The periodically varying contribution from valence electrons to the binding energy of a spherical sodium cluster. Magic numbers are indicated. Based on Ref. 9.

The experiments were performed with beams of free flying clusters produced by adiabatic expansion from a hot oven into vacuum. In the oven, argon or krypton gas at stagnation pressures of $(4-8) \times 10^5$ Pa is seeded with saturated sodium vapor at $700-800^\circ\text{C}$, i.e., partial sodium pressures of $(1-4) \times 10^4$ Pa. The diameter of the cylindrical expansion nozzle is 0.07 mm and its length about 0.15 mm. With the aid of skimmers and a differential pumping stage, the sodium cluster beam is introduced into a 3-m-long flight line. Ionization of the clusters is achieved by crossing the beam with a 2-mm-diam ray of ultraviolet light from a 1-kW xenon lamp. The photon energy is centered at 3.9 eV, with a bandwidth (FWHM) of 1.0 eV. This ensures an ionization probability that varies smoothly with size, and at the same time negligible heating of the ionized species.¹³ After ionization the clusters are analyzed by time-of-flight mass spectrometry to obtain the abundance variations as a function of size N . The flight time prior to analysis is typically 1 ms. The time-of-flight spectrometer consists of a 5-10-kV acceleration stage, deflection

plates that sweep the ionized dc beam across a narrow slit at about 3 kHz picking out narrow bunches with a well-defined starting time for the flight-time measurement, a reflectron to compensate for small velocity variations, and a channeltron ion detector. The arrival times are recorded with a multihit time-to-digital converter and passed to a computer that records the mass spectrum. The mass resolution is typically $\Delta M/M = 1200$. After background subtraction each mass peak is integrated to give the total mass abundance I_N .

The top panels in Fig. 2 show the measured abundance distributions I_N . On the left-hand side are results obtained with argon carrier gas; to the right, results with krypton gas. In both cases, the spectra have a bell-shaped envelope modulated by a sawtoothlike fine structure. The envelopes reflect the global kinetics of cluster growth during the high-pressure phases of the expansion, while the fine structure is interpreted^{1,14} as being due to shell structure (Fig. 1). We believe that the cluster condensation processes are likely to produce large clusters at near boiling temperatures, and that the sawtooth struc-

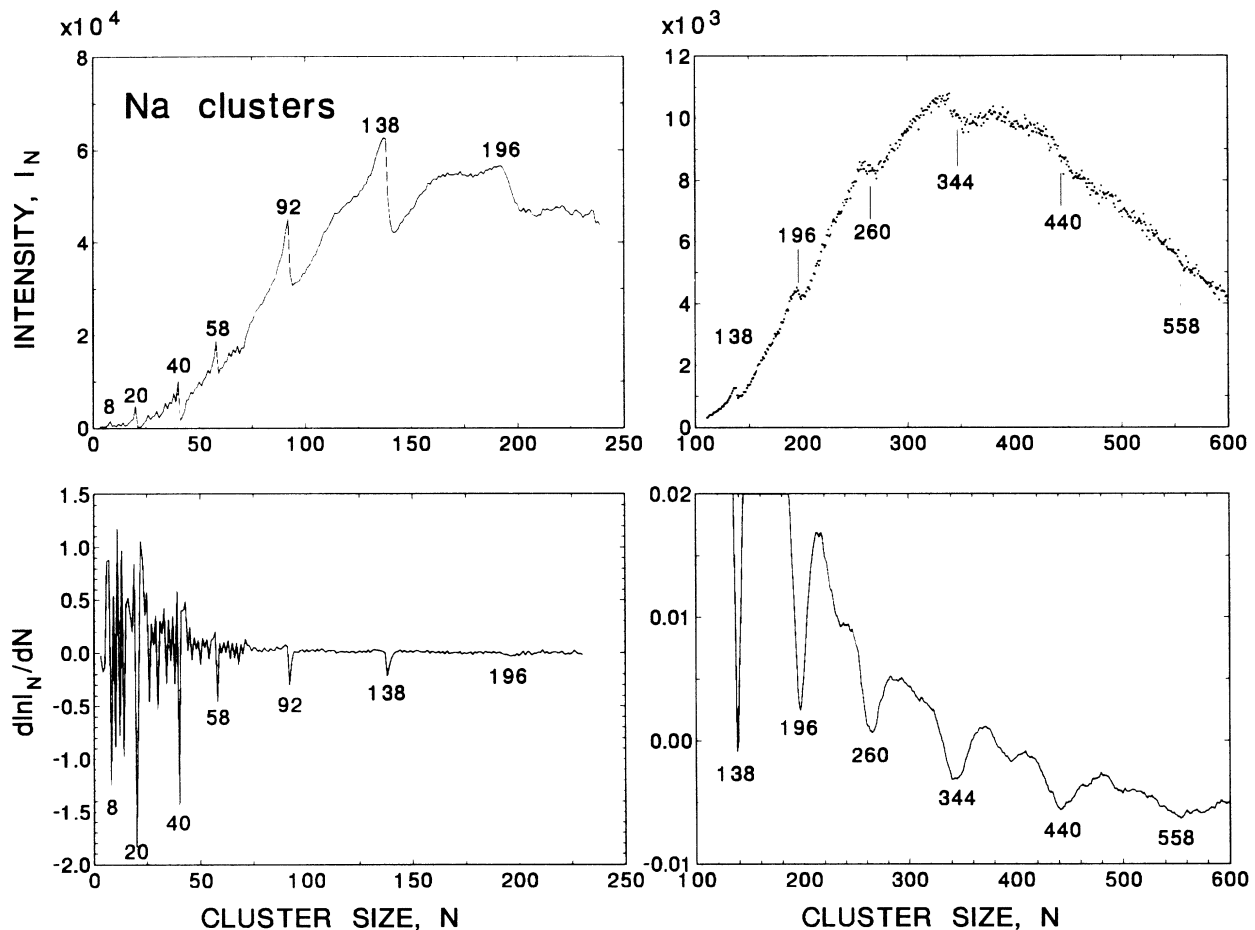


FIG. 2. Top panels: Abundance distributions for sodium clusters produced by adiabatic expansion and measured by time-of-flight mass spectrometry. Bottom panels: Logarithmic derivative of results in top panels. Bottom left, Eq. (1); bottom right, Eq. (2).

tures emerge as a result of subsequent evaporation and cooling in flight from isolated clusters.¹⁵ A given cooling time defines a definite temperature.^{15,16} In our case, 1 ms, it is estimated to be 300–400 K.

The sawtooth steps become gradually more rounded as one proceeds towards higher magic numbers (see, e.g., the step near $N=196$). With an increasing number of shells, confined to an energy interval about equal to the Fermi energy — 3.24 eV for Na—the gaps at the closed shells will diminish. At finite temperatures electrons can be excited across the gaps, and this tends to smear out the shell structure. Quantitative interpretations of the abundance spectra will require consideration of the thermodynamics of the electronic degrees of freedom, in addition to the ionic degrees of freedom, in estimating the free energies of monomer evaporation. Work along this

line is in progress.¹⁷

The local features of the abundance spectra can be displayed more clearly by taking the logarithmic derivative of the I_N values:

$$d \ln I_N / dN = 2(I_{N+1} - I_N) / (I_{N+1} + I_N). \quad (1)$$

The lower-left panel in Fig. 2 is a plot of this quantity. It eliminates the influence of the global shape. On the other hand, the above-mentioned smearing at higher shells tends to reduce the value of the logarithmic derivative strongly. This is compounded by the general decrease in relative magnitude of the sawtooth steps with increasing N . As a result, statistical uncertainties begin to obscure the shell effects. In the lower-right-hand panel we have plotted a generalized logarithmic derivative,

$$\left(\frac{d \ln I_N}{dN} \right)_W = \frac{\sum_{k=0}^{\infty} [2(I_{N+1+k} - I_{N-k}) / (I_{N+1+k} + I_{N-k})] \exp(-k^2/W^2)}{\sum_{k=0}^{\infty} (2k+1) \exp(-k^2/W^2)}, \quad (2)$$

with $W=6$ for size 100 increasing linearly to $W=36$ for size 600. Averaging over mass intervals W comparable to the smearing makes the shell dips stand out clearly again. The magic numbers determined experimentally in this way are indicated in Fig. 2 and in Table I. By comparison with Fig. 1 it is readily seen that the experimental shells also scale with the cube root of the cluster size, i.e., with the linear dimensions.

Any spherical binding field will have $2(2l+1)$ degenerate levels for each eigenvalue of l . The average spacing of these subshells scales with $N^{2/3}$. The $N^{1/3}$ periodicity, on the other hand, involves a bunching of several subshells with different l values. The precise values of the magic numbers will depend on the detailed shape of the radial potential. In Table I we compare experimentally determined shell closing with theoretical model predictions. The comparison shows that both experimentally and theoretically the positions of shell closings may vary from case to case, but the general $N^{1/3}$ scaling prevails.

This $N^{1/3}$ periodicity is characteristic of a constant-

TABLE I. Magic numbers describing spherical shell closures in metal clusters. LDA denotes local-density approximation.

Shell n	Experiment			Theory (Na)		
	Ag ^a	Au ^a	Cs ^b	Na ^c	Woods-Saxon ^d	Jellium LDA ^e
0	2	2	2	2	2	2
1	8	8	8	8	8	8
2	20	20	18/20	20	20	18/20
3	40	34	34/40	40	40	34/40
4	58	58	58	58	58	58
5	92	...	92	92	92	92
6	138	...	138	138	138	138
7	(198)	...	198 ± 2	196	198	186/196
8			263 ± 5	260 ± 4	254/268	254
9			341 ± 5	344 ± 4	338	338
10			443 ± 5	440 ± 2	440	440
11			557 ± 5	558 ± 8	562	556
12			700 ± 15		694	676
13			840 ± 15		832	832
14			1040 ± 15		1012	

^aReference 4.

^bReferences 3 and 18 and T. P. Martin (private communication).

^cThis work.

^dReference 9.

^eReference 17.

density, weak-field medium confined by a more or less steeply rising spherical surface potential,⁹ but it is not unique. A classical packing model can also give rise to closed, shell-like configurations with magic numbers that scale with $N^{1/3}$, as shown, for example, by Miehle *et al.* with Xe clusters.¹⁹ The quantal origin of the presently observed shells, Fig. 2, is first of all suggested by the close agreement with the calculations in Fig. 1. In addition, the following simple considerations support a quantal interpretation. If the sodium droplets all have the same density, their radii are equal to $R = r_{WS}N^{1/3}$, where r_{WS} is the Wigner-Seitz radius.²⁰ Inserting the six highest magic numbers N_0 from Fig. 2 shows that there is an increment in radius of $\Delta R = (0.61 \pm 0.02)r_{WS}$ each time a new shell is added. Such a small increment is hardly compatible with a packing model, where each shell represents an atomic layer. Instead one may compare the Fermi wavelength of electrons in simple metals, $\lambda_F = (32\pi^2/9)^{1/3}r_{WS} = 3.28r_{WS}$, with the increment in the length ΔL of a peripheral circular orbit, $2\pi\Delta R = (3.83 \pm 0.12)r_{WR}$. This agreement already supports a quantal origin of the observed shell structure. As a further step one may compare⁹ with a triangular orbit, $\Delta L = 3\sqrt{3}\Delta R = (3.17 \pm 0.10)r_{WS}$, or with a square orbit $\Delta L = 4\sqrt{2}\Delta R = (3.45 \pm 0.01)r_{WS}$. The two values bracket the Fermi wavelength. In semiclassical terms⁹ one may thus visualize a shell in terms of the increase in surface radius required to give room for an extra node in stationary waves of approximately triangular or square shapes.

Summarizing, we have shown experimentally that the mean-field, independent-particle model used to describe atoms and nuclei can be extended to sodium metal clusters containing many hundreds of conduction electrons. Each spherical shell comprises several l values, and a new shell closing appears whenever the radius of the cluster has been incremented by a characteristic length, equal to about 0.6 times the Wigner-Seitz radius.

There is no reason to believe that the present experiments with up to 600 electrons in a cluster have reached an upper limit for the occurrence of quantal shell structure. The perspective of extending experiments to clusters with several thousand electrons appears to be open.²¹ One interesting possibility is the study of large-scale modulations of the shell structure (supershells⁹) as shown in Fig. 1.

Special thanks are due to W. D. Knight for guiding the authors into the field of experimental cluster research during a sabattical stay at the Niels Bohr Institute.

Theoretical discussions with M. Brack, B. R. Mottelson, and H. Nishioka are gratefully acknowledged. We also thank D. Radford for developing our peak fitting program. This work has been supported by The Carlsberg Foundation, The Danish Research Academy, The Danish National Science Research Council, Julie Damm's Fund, Novo's Fund, SARC Fund, and Thomas B. Thriges Fund. The authors are grateful to W. A. de Heer and W. D. Knight for detailed advice on the construction of the cluster machine.

^(a)Present address: Physics Department, University of New Hampshire, Durham, NH 03834.

¹W. D. Knight, K. Clemenger, W. A. de Heer, W. A. Saunders, M. Y. Chou, and M. L. Cohen, *Phys. Rev. Lett.* **52**, 2141 (1984).

²K. Clemenger, Ph.D. thesis, University of California, Berkeley, 1985 (unpublished).

³T. Bergmann and T. P. Martin, *J. Chem. Phys.* **90**, 2848 (1989).

⁴I. Katakuse, T. Ichihara, Y. Fujita, T. Matsuo, T. Sakurai, and H. Matsuda, *Int. J. Mass Spectrom. Ion Processes* **67**, 229 (1985).

⁵W. Ekardt, *Phys. Rev. B* **29**, 1558 (1984).

⁶O. E. Beck, *Solid State Commun.* **49**, 381 (1984).

⁷M. Y. Chou and M. L. Cohen, *Phys. Lett. A* **133**, 420 (1986).

⁸M. G. Mayer and J. H. D. Jensen, *Elementary Theory of Nuclear Shell Structure* (Wiley, New York, 1955).

⁹H. Nishioka, K. Hansen, and B. R. Mottelson, *Phys. Rev. B* (to be published).

¹⁰S. Bjørnholm, *Contemp. Phys.* (to be published).

¹¹R. Balian and C. Bloch, *Ann. Phys. (N.Y.)* **69**, 76 (1971).

¹²A. Bohr and B. R. Mottelson, *Nuclear Structure II* (Benjamin, London, 1975).

¹³W. A. de Heer, Ph.D. thesis, University of California, Berkeley, 1985 (unpublished).

¹⁴W. A. de Heer, W. D. Knight, M. Y. Chou, and M. L. Cohen, *Solid State Phys.* **40**, 93 (1987).

¹⁵C. E. Klots, *J. Chem. Phys.* **92**, 5864 (1988).

¹⁶C. Brechignac, Ph. Cahuzac, J. Leygnier, and J. Weiner, *J. Chem. Phys.* **90**, 1492 (1989).

¹⁷M. Brack, O. Genzken, and K. Hansen (to be published).

¹⁸T. P. Martin, T. Bergmann, H. Göhlich, and T. Lange, *Phys. Rev. Lett.* **65**, 748 (1990).

¹⁹W. Miehle, O. Kandler, T. Leisner, and O. Echt, *J. Chem. Phys.* **91**, 5940 (1989).

²⁰N. W. Ashcroft and N. D. Mermin, *Solid State Physics* (Saunders College, Philadelphia, 1976).

²¹T. P. Martin has recently reported on measurements of Na clusters up to several thousand (private communication).